NAFTA-GAZ

Nafta-Gaz 2024, no. 9, pp. 531–550, DOI: 10.18668/NG.2024.09.01

Modeled and empirical approaches to evaluate rock petrophysics parameters: a case study of Dhodak Gas Field, Pakistan

Modelowe i empiryczne podejście do oceny parametrów petrofizycznych skał na przykładzie złoża gazu Dhodak w Pakistanie

Sarfraz Khan[1], Shuja Ullah[1,*], Umair B. Nisar[2], Waqas Ahmed[1], Muhammad R. Mughal[3], Irfan[1], Shahid Nawaz[1], Nazir ur Rehman[4]

[1]*National Centre of Excellence in Geology, University of Peshawar*
[2]*Centre for Climate Research and Development, COMSATS University Islamabad*
[3]*Department of Meteorology, COMSATS University Islamabad*
[4]*Department of Geology, Khushal Khan Khattak University Karak*

ABSTRACT: The main aim of the presented study was to perform an analysis of petrophysical rock parameters for the Pab Formation, which is a potential reservoir, located at four-depth intervals within the Dhodak Gas Field. The Pab Formation in the studied wells is mostly composed of the well-sorted sandstone. The intervals for the study were selected by applying a gamma ray log cut-off of 40%. A Matlab code that is user-friendly and contains empirical and numerical models (Raymor's, Han's, Castagna's, Jizba, Blangy, and Gardner's models) was designed with the purpose of providing an interpretation of rock physics parameters in reservoirs. The results indicate that the Pab Formation is mainly saturated with hydrocarbons and possesses sufficient porosity (i.e. between 8 and 38%). According to the cross-plot models, there are a few zones within the Pab Formation that are weakly consolidated. These zones are located at depths of 2377–2404 m and 2418–2430 m. However, the same area is classified as tight gas sandstone and is located between 2330 to 2343 m. The results of the study indicate that the Pab Formation is potentially saturated with hydrocarbons. These findings were based on structural and rock physics assessments of the study area. The approach presented in this work is also helpful for structural trap evaluation. In addition, the petrophysical rock parameter models developed can contribute to reducing the risks associated with hydrocarbon exploration, enabling accurate representation of subsurface conditions and improving reservoir forecasting capabilities in oil producing areas.

Key words: rock petrophysics parameters, empirical models, MATLAB coding, crossplots, Middle Indus basin.

STRESZCZENIE: Głównym celem prezentowanych badań było przeprowadzenie analizy parametrów fizycznych skał dla serii piaskowcowej Pab, która jest potencjalną skałą zbiornikową, zalegającą w czterech interwałach głębokościowych w obrębie złoża gazu Dhodak. Formacja Pab w analizowanych odwiertach zbudowana jest głównie z dobrze wysortowanych piaskowców. Interwały do badań zostały wybrane poprzez zastosowanie odcięcia na profilowaniu gamma na poziomie 40%. Kod Matlab, który jest przyjazny dla użytkownika i zawiera modele empiryczne i numeryczne (modele Raymora, Hana, Castagny, Jizby, Blangy'ego i Gardnera), został zaprojektowany w celu umożliwienia interpretacji parametrów petrofizycznych skał. Wyniki wskazują, że piaskowiec Pab jest głównie nasycony węglowodorami i ma zadowalającą porowatość (tj. pomiędzy 8 a 38%). Na podstawie analizy wykresów krzyżowych stwierdzono, że istnieje kilka stref w obrębie formacji Pab, które są słabo skonsolidowane. Strefy te lokalizowane zostały w głębokościach 2377–2404 m i 2418–2430 m. Jednak w tym samym rejonie występuje piaskowiec gazonośny (o charakterze *tight gas*) znajdujący się na głębokości 2330–2343 m. Wyniki przeprowadzonych badań wskazują, że piaskowiec Pab może być potencjalnie nasycony węglowodorami. Ustalenia te oparto na ocenie strukturalnej oraz ocenie parametrów petrofizycznych skał w obszarze badań. Podejście przedstawione w tej pracy jest również pomocne do oceny pułapek strukturalnych. Ponadto opracowane modele parametrów petrofizycznych skał mogą się przyczyniać do zmniejszenia ryzyka związanego z poszukiwaniami węglowodorów, umożliwiając dokładne odwzorowanie warunków panujących pod powierzchnią i poprawiając możliwości prognozowania złóż w obszarach wydobycia ropy naftowej.

Słowa kluczowe: parametry petrofizyczne skał, modele empiryczne, kodowanie MATLAB, crossploty, basen środkowego Indusu.

Corresponding author: S. Ullah, e-mail: *shujageo@gmail.com*

Article contributed to the Editor: 07.03.2024. Approved for publication: 11.09.2024.

Introduction

Rock physics has been playing its part in theoretical modeling and laboratory analysis since the development of oil and gas fields. It has extended its roots, being an essential part of well logs, and seismic and electromagnetic data analysis. It has become a significant tool of reservoir geophysics and an integral part of quantitative seismic interpretation (Avseth et al., 2010; Souza and Rostirolla, 2011). Nowadays it is a mandatory part of basin characterization which is highlighted in recent research studies (Khan et al., 2015; Lie, 2016; Okwu and Nwachukwu, 2019). The rock physics tool can reduce uncertainty in seismic exploration and enhance reservoir forecasting in the petroleum industry (Draege et al., 2006). Avseth et al. (2010) highlighted the importance and benefit of linking rock physics parameters to geologic processes, including depositional and diagenetic trends. Scientific programming provides this link by integrating several mathematical relations and matrices to increase data reliability (da Veiga et al., 2014; Okwu and Olufemi, 2018; Boah et al., 2019).

Scientific programming has introduced a new dimension in hydrocarbon exploration. Several computing environments (Fotran, C^{++}, MATLAB, Python) are available for the users to transform theory into practical applications which can be used in the development of tools for a better understanding of subsurface conditions (Kearey et al., 2002).

MATLAB among all the available languages is the easiest and most productive computing environment for scientists (Moore, 2009). Despite the evolution of Python, the importance of MATLAB has not decreased. The application of MATLAB in empirical/numerical analysis has been extensively used by Cao et al. (2010). These scientists utilized MATLAB computational studies in identifying/delineating the subsurface structural features. Emujakporue et al. (2012), Agbauduta (2014), and Margrave and Lamoureux (2019) used this technique to correlate seismic, well log, and petrophysical parameters. Amit and Zhiling (2012) and Bhaskar et al. (2013) have used this computation to carry out seismic attribute analysis at the reservoir level whereas Forth (2006) has used MATLAB for correlations of different rock physics parameters in delineating the reservoir.

The scope of the proposed research is to assess hydrocarbon potential and understand rock physics trends in Pab Formation in the Dhodak field by superimposing the modeled and actual results using MATLAB. The results will highlight cross-plot models for the identification of potential hydrocarbon prospect intervals in the Dhodak-03 well.

The study will not only help to assess the different empirical relationships but will also depict their working under different reservoir conditions.

Geological setting

The Dhodak Field is located in the eastern part of the Sulaiman Range, Middle Indus basin (Nazeer et al., 2013; Mahmood et al., 2017). On its northern flank, 2–5 km Zinda Pir Anticlinorium is exposed and surrounded by north-south thrust fault features (Figure 1). The steep dipping limbs of this anticlinorium progressively become gentle towards the base of the Eocene core. A vertical to sub-vertical east-west trending strike-slip Zarwan fault is located parallel to the axial trend of this anticlinorium. In the northern part, echelon nappes with tightly folded synclines are present (Moghal et al., 2007). The southern ridge is formed by an anticline which is flanked by a northward verging syncline on the southern limb. Some structural features are exposed on the surface and marked on geo-referenced satellite images e.g., the left lateral Kingri fault which marks the western boundary of the Dhodak field and the Choudwan fault limits the Eastern margin. The study area has a key significance in hydrocarbon exploration over the past few decades (Naseer et al., 2007) with an average daily production of 42 MMSCFT of gas, 2600 barrels of condensate, and 180 tons of Liquid Petroleum Gas (LPG) (Humayon et al., 2012). The eastern part of the Sulaiman Range is mainly a light oil-condensate province, while the central Sulaiman Range is dominantly a gas province. For the petroleum geology aspect, two nearby formations (Pab Formation and Chiltan Limestone) may be considered as possible reservoir rocks for this hydrocarbon generation. The petroleum play comprises of the Ranikot Sandstone being the main reservoir. In addition to that, Pab Formation as well as Mughal Kot Formation are the potential reservoir rocks, the Cretaceous Sembar Formation is the dominant source rock in the study area whereas Ghazij shale acts as a seal rock. The whole stratigraphic succession in the study area and its surroundings ranges in age from Triassic (Wulagai Formation) to recent (Lei conglomerate) (Ullah et al., 2006; Ullah et al., 2022).

Methodology and data set

Crossplot analysis in rock physics indicates the variation of the petrophysics parameters depending on reservoir fluid saturation and lithology. Rock physics crossplots based on the log measurements for each well were evaluated to better define the relationship between elastic parameters and rock properties, such as lithology and saturation. For widespread sedimentary rocks, different empirical correlations exist between the distinct elastic properties and reservoir properties i.e., (a) Gardner's relation between density and velocity, (b) Han's relation between *P*-wave velocity and porosity,

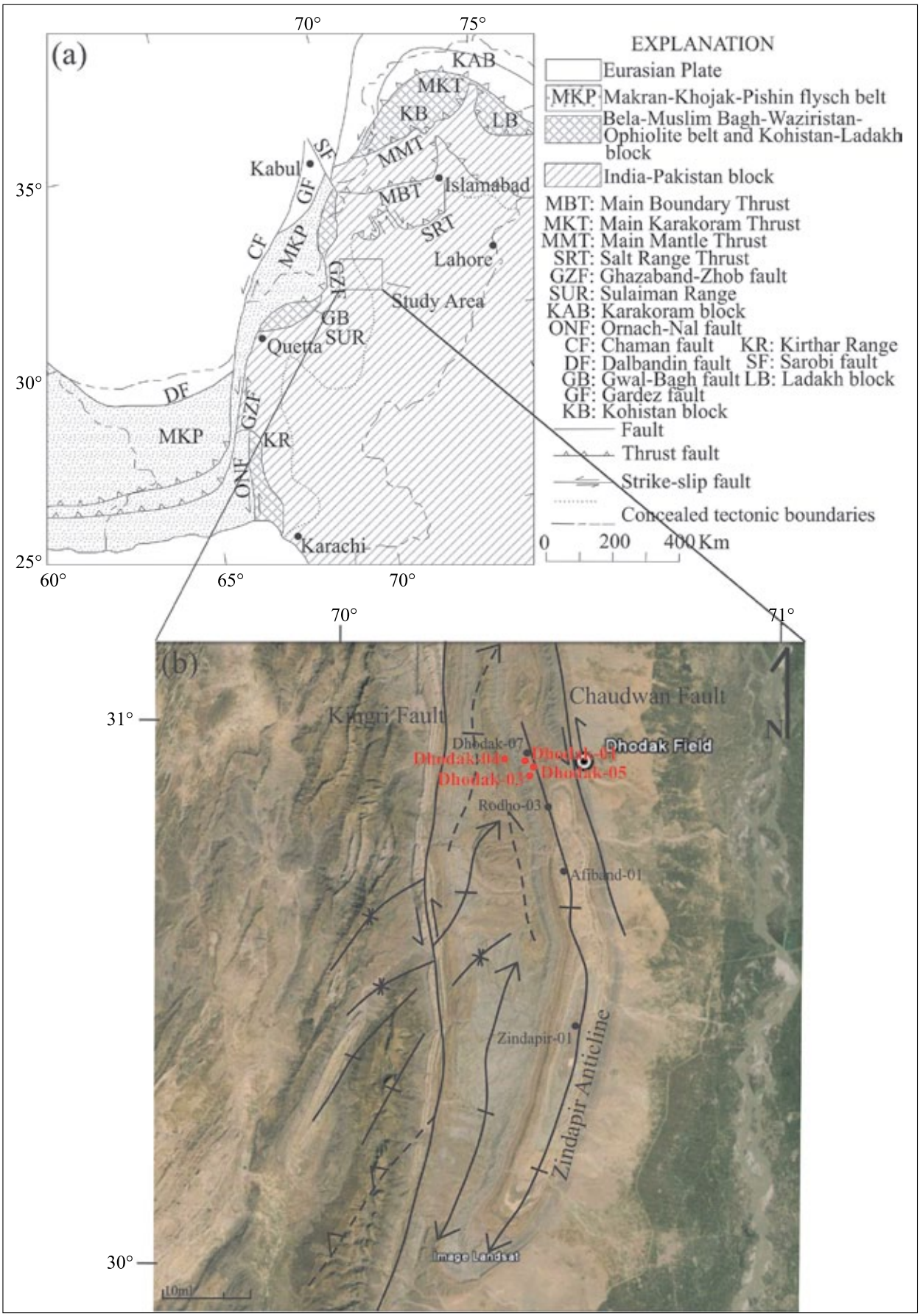

Figure 1. a) Regional geological settings of Pakistan; b) A location map of the study area – Dhodak field area, Middle Indus basin

Rysunek 1. a) Regionalny szkic geologiczny Pakistanu; b) Mapa sytuacyjna obszaru badań – rejon złoża Dhodak, basen Środkowego Indusu

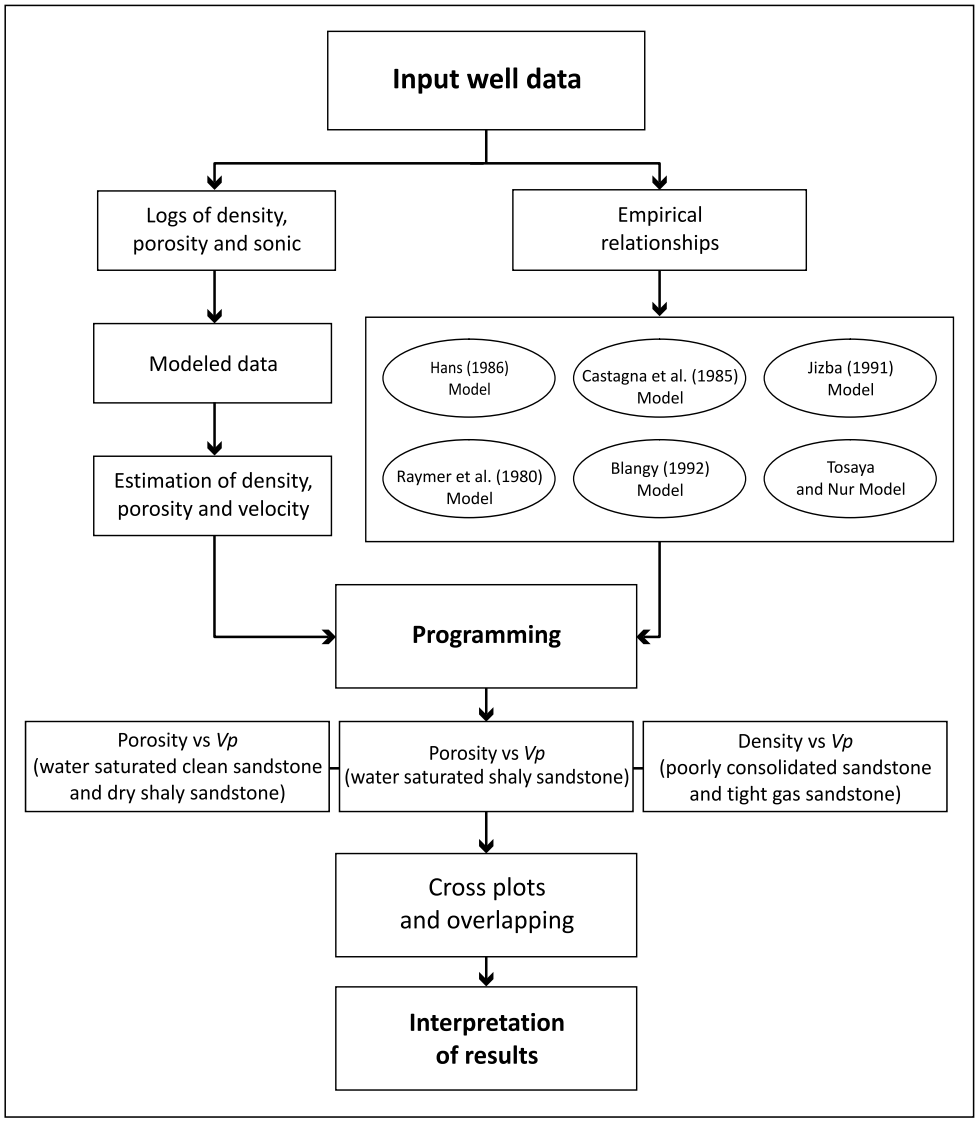

Figure 2. Methodology flow chart for the studies performed
Rysunek 2. Schemat metodologii dla wykonanych badań

and (c) Raymer's relation between velocity and porosity with different mineral and fluid content.

To create petrophysical parameter models or empirical relationships, the work of Mavko et al. (2009) and available well log data were used. The authors applied data in LAS format (sonic, density, and neutron logs) from the following wells: Dhodak-01, -03, -04, and -05. The standard empirical relations/models are then applied to analyse the available well log data (Figure 2).

Following the acquisition of the requisite derived data, bespoke programs have been devised in MATLAB (a programming language), the well log data has been plotted, and rock physics models have been superimposed on the plotted data, thereby obtaining the requisite cross plots.An analysis is carried out for Pab Formation (Cretaceous age) in Dhodak-01, -03, -04, and -05 wells. The two data types i.e., log data and modeled data are discussed below.

Well log data

The well log data from Dhodak-01, -03, -04, and -05 wells (Figures 3–5) were used to analyse the profile of the Pab Formation. Different parameters were calculated by using different logs such assonic log (for Vp and porosity calculation), density log (for bulk density and porosity calculation), and neutron log (for porosity calculation).

Empirical Models

In practice, standard empirical relations or rock physics models are often used. The approaches for empirical models are simple, some function forms are assumed and then the empirical coefficients are determined by calibrating a regression over the data. A two-step process is involved in all the empirical relations (Gardner et al., 1974; Raymer et al., 1980; Castagna et al., 1985; Han, 1986; Jizba, 1991; Blangy, 1992) for modeling. The procedure is to determine the functional

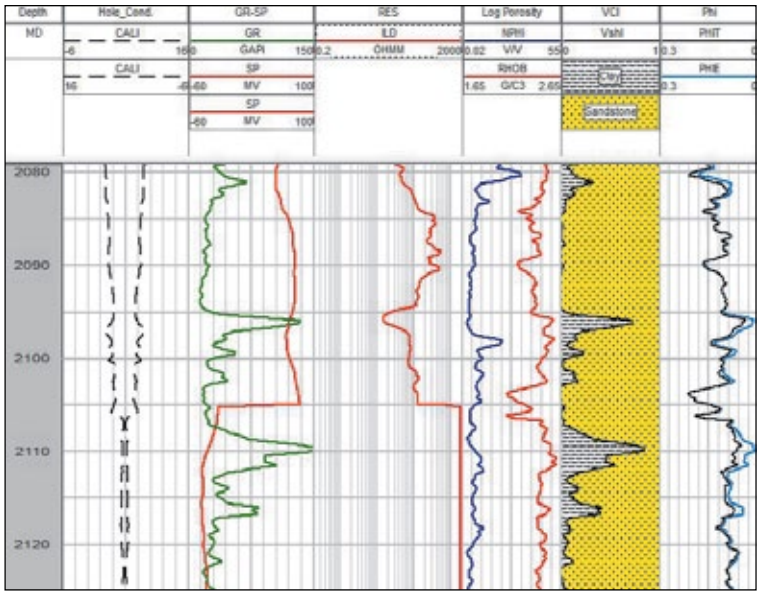

Figure 3. Basic well log interpretation for Dhodak-01 well

Rysunek 3. Interpretacja podstawowych profilowań geofizyki otworowej dla odwiertu Dhodak-01

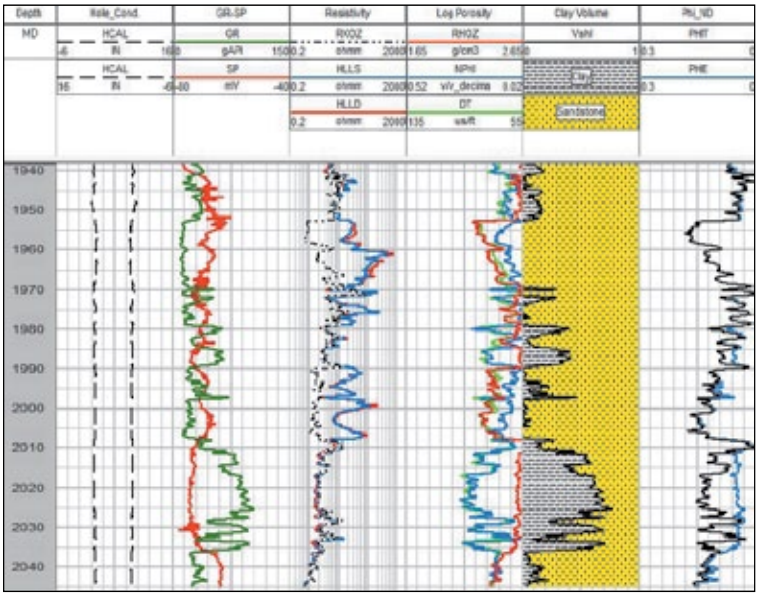

Figure 4. Basic well log interpretation for Dhodak-04 well

Rysunek 4. Interpretacja podstawowych profilowań geofizyki otworowej dla odwiertu Dhodak-04

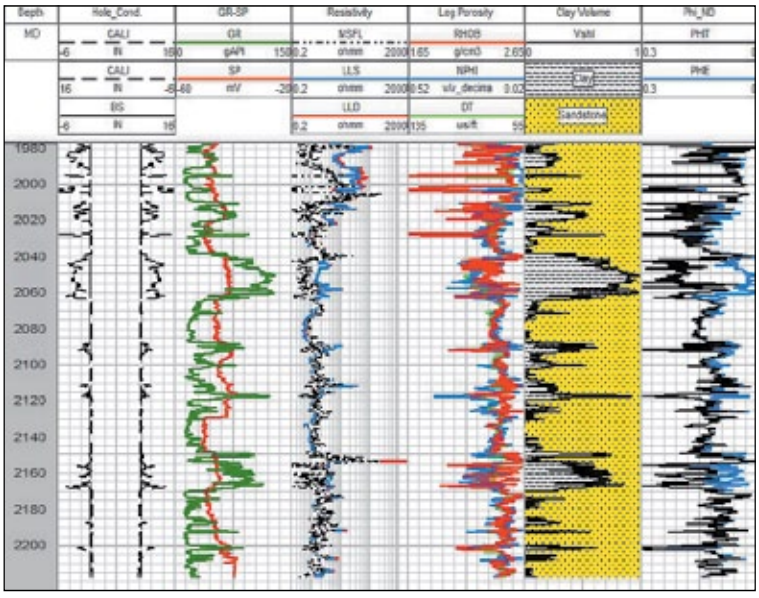

Figure 5. Basic well log interpretation for Dhodak-05 well

Rysunek 5. Interpretacja podstawowych profilowań geofizyki otworowej dla odwiertu Dhodak-05

form followed by a calibration step to determine the empirical coefficients. These relations are applied on well log data as a result of which a new modeled data for the area is obtained. This modeled data is then used in combination with log data for specific formations or zones of a formation and plots were generated in MATLAB and results were compared.

Some of the empirical models used in this research project are taken from Mavko et al. (2009) and are given below in detail:

Han's model

This model gives the relation between ultrasonic velocities to porosity and clay content based on laboratory works.

For water-saturated clean sandstones at 40 MPa, the equation (1) is:

$$Vp = 6.08 - 8.06\emptyset \quad (1)$$

where:
Vp – is P-wave velocity [km/sec],
$\emptyset$ – is porosity [%].

For water-saturated shaly sandstone, the correlation in equation (1) between velocity and porosity became relatively poor, which could become accurate if clay volume is included in the regression.

For water-saturated shaly sandstone at 40 MPa, the equation (2) is:

$$Vp = 5.59 - 6.96\emptyset - 2.18C \quad (2)$$

where:
Vp – is P-wave velocity [km/sec],
$\emptyset$ – is porosity [%],
C – is clay constant.

For dry shaly sandstones Han's empirical relation (2) obtains the form:

$$Vp = 5.41 - 6.35\emptyset - 2.87C \quad (3)$$

where:
Vp – is P-wave velocity [km/sec],
$\emptyset$ – is porosity [%],
C – is clay constant.

Tosaya and Nur model

This model obtained empirical regressions from ultrasonic (laboratory) measurements and found relations between velocities, porosity, and clay content for water-saturated shaly sandstones at an effective pressure of 40 MPa.

They cannot be adjusted for any other pore fluid, the relationship (4) is:

$$Vp = 5.8 - 8.6\emptyset - 2.4C \quad (4)$$

where:
Vp – is P-wave velocity [km/sec],
$\emptyset$ – is porosity [%],
C – is clay constant by volume.

Castagna's model

Castagna et al. (1985) determined empirical regression on the basis of log measurements, relating velocities with porosity and clay content under water-saturated conditions.

For shaly water-saturated sands, equation (5) is:

$$Vp = 5.81 - 9.42\emptyset - 2.21C \quad (5)$$

where:
$\emptyset$ – is the porosity,
C – is the clay volume fraction,
Vp – is the P-wave velocity [km/sec].

Raymer–Hunt–Gardner model

This model improved the Wyllie's empirical velocity-to-travel time (if the porosity is <37%) relation (6) as follows:

$$Vp = (1 - \emptyset)^2 V_m + V_f\emptyset \quad (6)$$

where:
Vp – represent rock velocity [km/sec],
V_m and V_f – are velocities [km/sec] of rock matrix and pore fluid respectively.

Jizba's model

This model performed controlled field and laboratory measurements and found an empirical relationship (7) between density and velocity for tight gas sandstones:

$$\rho = 1.96 + 0.117Vp \quad (7)$$

where:
ρ – is the density [g/cm^3],
Vp – is P-wave velocity [km/s].

Jizba's relation is good for sandstones while coals and evaporates can be off significantly from the expected behavior.

Blangy's model

Blangy (1992) found an empirical relationship (8) between density and velocity for poorly consolidated sandstone:

$$\rho = 1.498 + 0.224Vp \quad (8)$$

where:
ρ – is the density [g/cm^3],
Vp – is P-wave velocity [km/s].

Results and discussions

In the study area, rock physics analysis is carried out to determine lithology and fluid discrimination by employing different rock physics models/empirical models on the cross plots based on the well log data. Three to five zones in the profile of Pab Formation were analyzed in Dhodak-01, -03, -04, and

-05 wells by using different rock petrophysics models for the three parameters: porosity, velocity, and density, and the two data sets i.e., log data and modeled data.

Velocity-Porosity cross plot

An example plot of *P*-wave velocity vs porosity for a set of log data for various zones defined according to 40% of Gamma Ray cut-off may be found in Figures 6–9. In Dhodak-01, three zones are marked. In the analysis average volume of shale, average total porosity, and average effective porosity results as 10%, 12%, and 11% respectively for zone 1, 21%, 11%, and 10% respectively for zone 2, and 10%, 8% and 7% respectively for zone 3. In Dhodak-03, four zones are marked. In the analysis, the average volume of shale, average total porosity, and average effective porosity results are 35%, 14%, and 9% respectively for zone 1, 36%, 17%, and 11% (zone 2), 38%, 20% and 12% (zone 3) and 40%, 30% and 18% (zone 4). In Dhodak-04 and 05, five zones are marked. In Dhodak-04, the average volume of shale, average total porosity, and average effective porosity results are 6%, 11%, and 9% respectively for zone 1, 14%, 15%, and 12% (zone 2), 8%, 14% and 13% (zone 3), 19%, 9% and 7% (zone 4), and 3%, 13%, and 12% (zone 5). In Dhodak-05, the average volume of shale, average total porosity, and average effective porosity results are 5%, 8%, and 8% respectively for zone 1, 8%, 3%, and 3% (zone 2), 10%, 6% and 6% (zone 3), 5%, 11% and 11% (zone 4), and 23%, 12%, and 9% (zone 5). In these crossplots, there is a general trend of velocity decreasing with porosity.

Two empirical models i.e., Han's (for dry shaley sandstone) and Raymer's (for water-saturated clean sandstone) are superimposed on the plotted log data. Both of the models deviate from the data and underestimate the plotted data. Raymer's model failed because the zones were not clean and had clay contents of 34% to 38%. This underestimation by Han's model is due to the presence of fluids meaning that these parts of the formation are either saturated with water or oil (Gardner et al. 1974; Han 1986).

Three other models i.e., Han's, Tosaya's, and Castagna's model, for water-saturated shaley sandstone with 5% clay contents were also applied and superimposed on the log data with the assumption that the rock is water-saturated (Figures 10, 11, 12, and 13). These models also underestimate the data and do not produce satisfactory results. This underestimation is caused by the assumption that the rock is water-saturated which shows that the zones in each well are not water-saturated but rather hydrocarbon saturated. The results indicate that these zones are hydrocarbon-bearing zones which is a good insignia in the classification of the reservoir as a potential hydrocarbon producer (Gardner et al. 1974; Han 1986; Castagna et al. 1994).

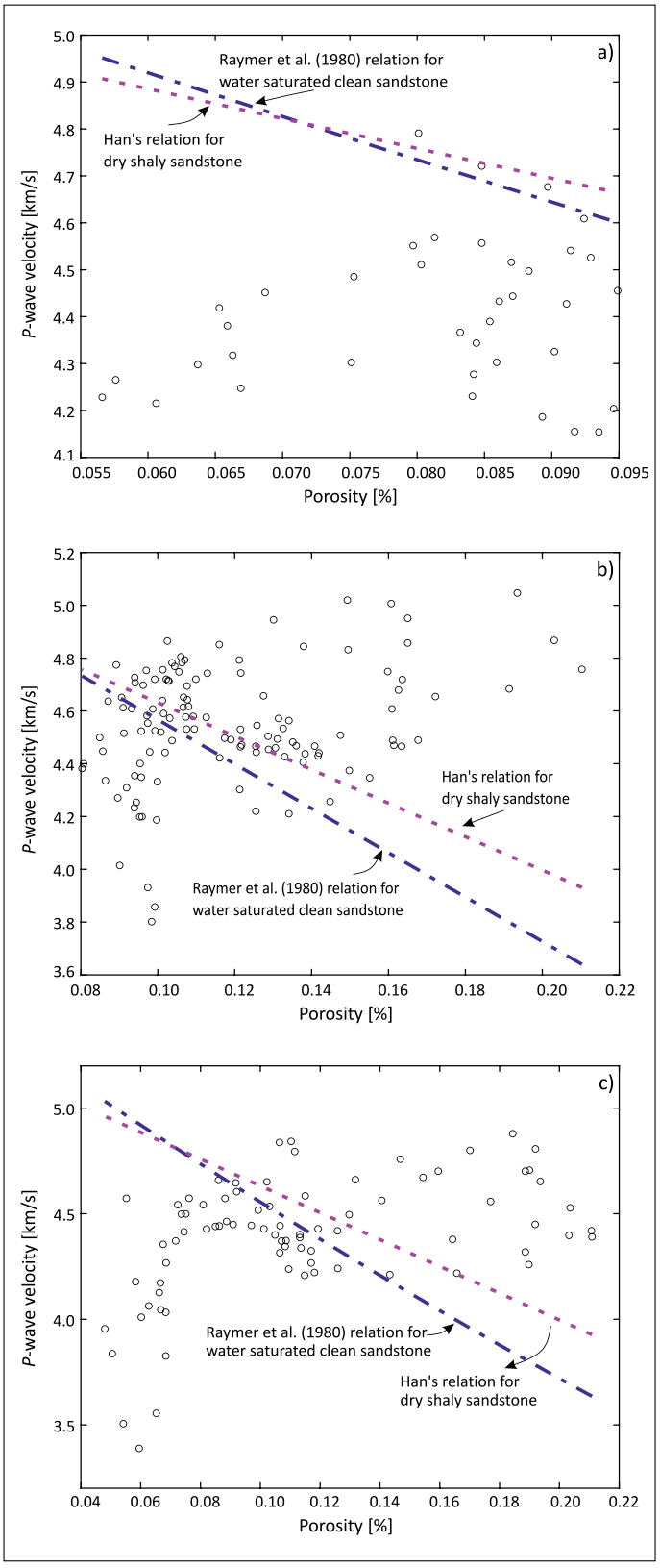

Figure 6. Velocity vs porosity crossplot of Dhodak-01 for a) zone 1 (2080–2095 meters), b) zone 2 (2100–2110 meters), and c) zone 3 (2120–2124 meters) with derived data (blue and purple lines)

Rysunek 6. Wykres krzyżowy prędkości i porowatości dla a) strefy 1 (2080–2095 m), b) strefy 2 (2100–2110 m) i c) strefy 3 (2120–2124 m) z danymi pochodnymi (linie: niebieska i fioletowa) – otwór Dhodak-01

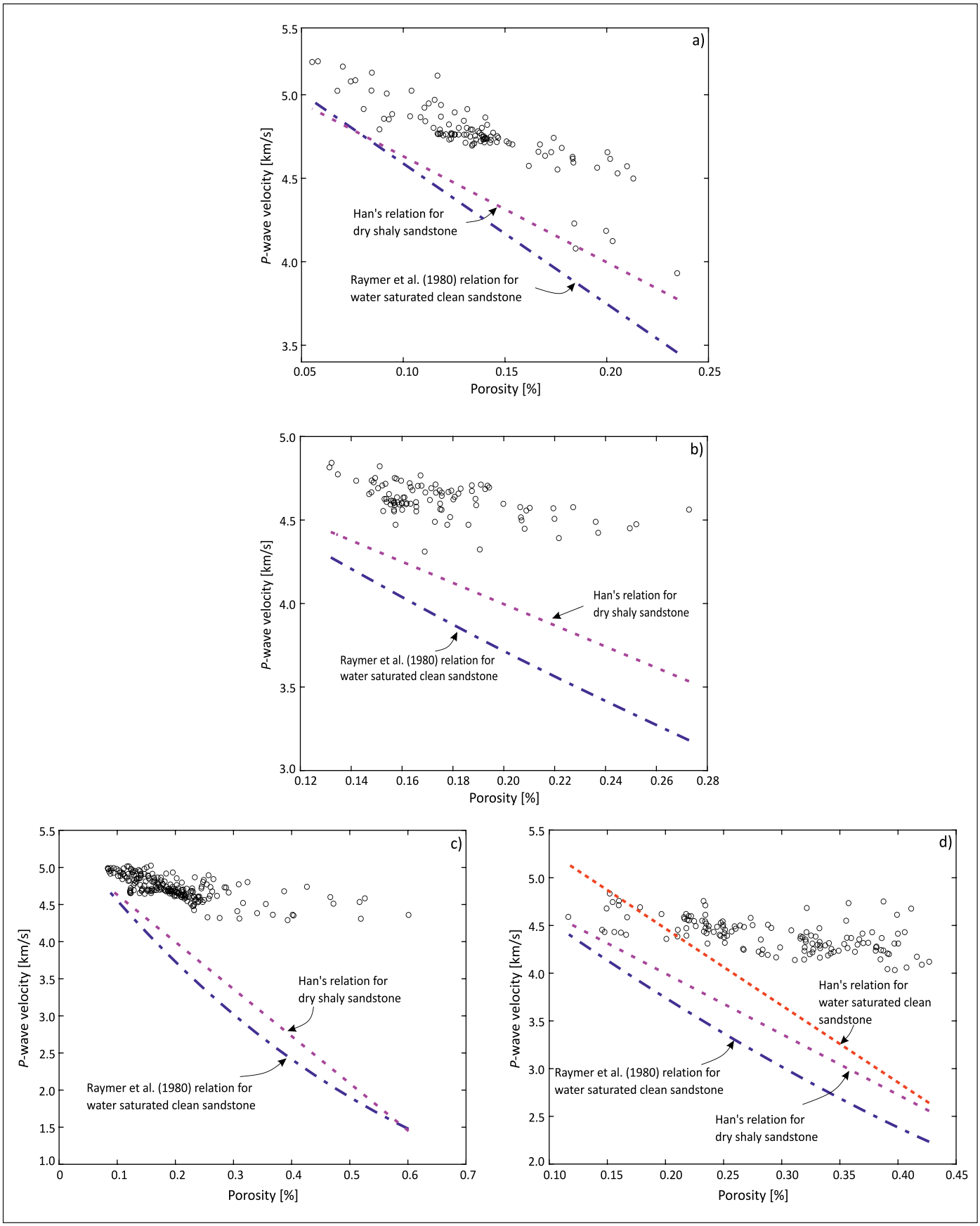

Figure 7. Velocity vs porosity crossplot of Dhodak-03 for a) zone 1 (2330–2343 meters), b) zone 2 (2352–2364 meters), c) zone 3 (2377–2404 meters), and d) zone 4 (2418–2450 meters) with derived data (blue and purple lines)

Rysunek 7. Wykres krzyżowy prędkości i porowatości dla a) strefy 1 (2330–2343 m), b) strefy 2 (2352–2364 m), c) strefy 3 (2377–2404 m) i d) strefy 4 (2418–2450 m) z danymi pochodnymi (linie: niebieska i fioletowa) – otwór Dhodak-03

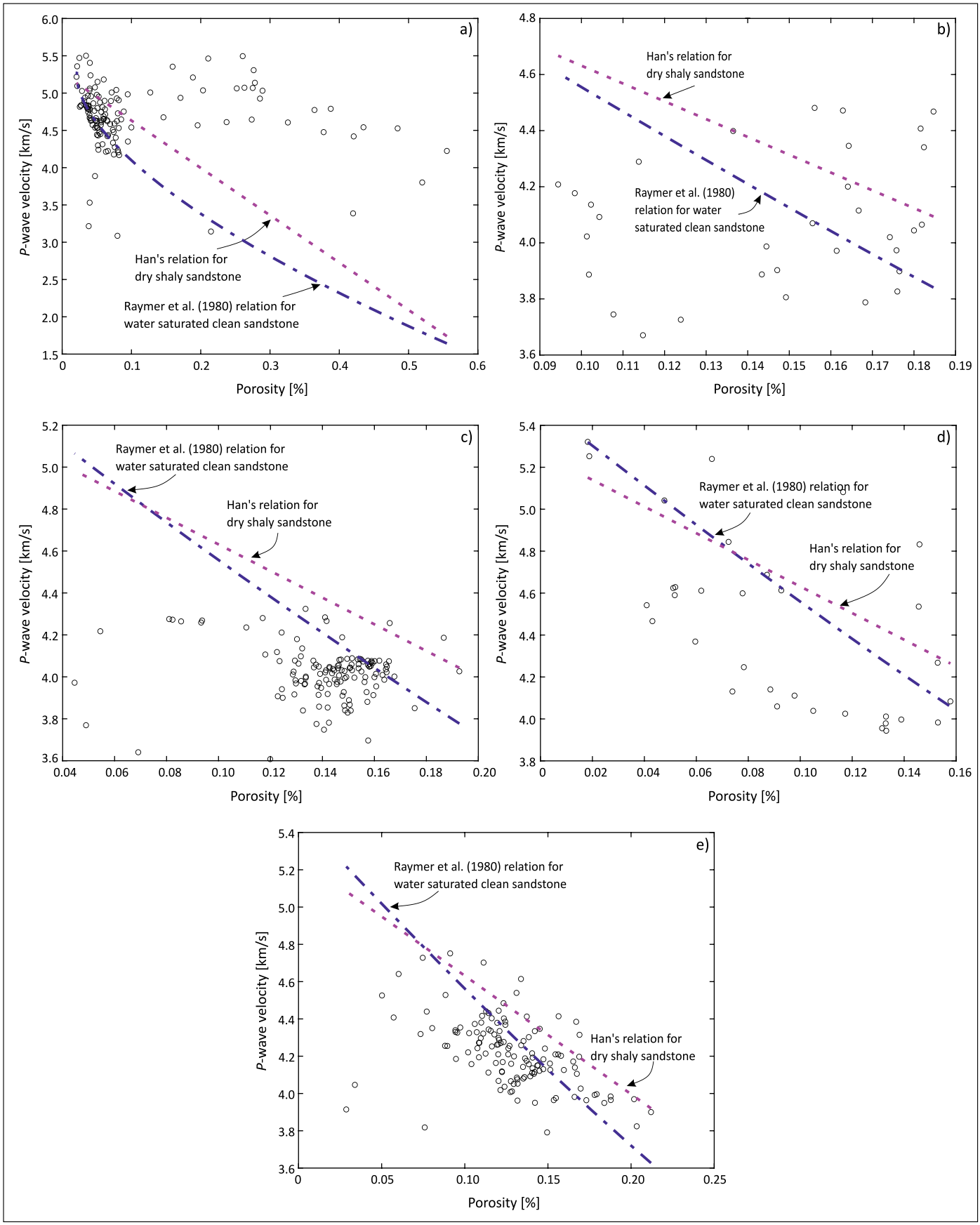

Figure 8. Velocity vs porosity crossplot of Dhodak-04 for a) zone 1 (1990–2010 meters), b) zone 2 (2020–2025 meters), c) zone 3 (2070–2090 meters), d) zone 4 (2110–2115 meters), and e) zone 5 (2125–2145 meters) with derived data (blue and purple lines)

Rysunek 8. Wykres krzyżowy prędkości i porowatości dla a) strefy 1 (1990–2010 m), b) strefy 2 (2020–2025 m), c) strefy 3 (2070–2090 m), d) strefy 4 (2110–2115 m) i e) strefy 5 (2125–2145 m) z danymi pochodnymi (linie: niebieska i fioletowa) – otwór Dhodak-04

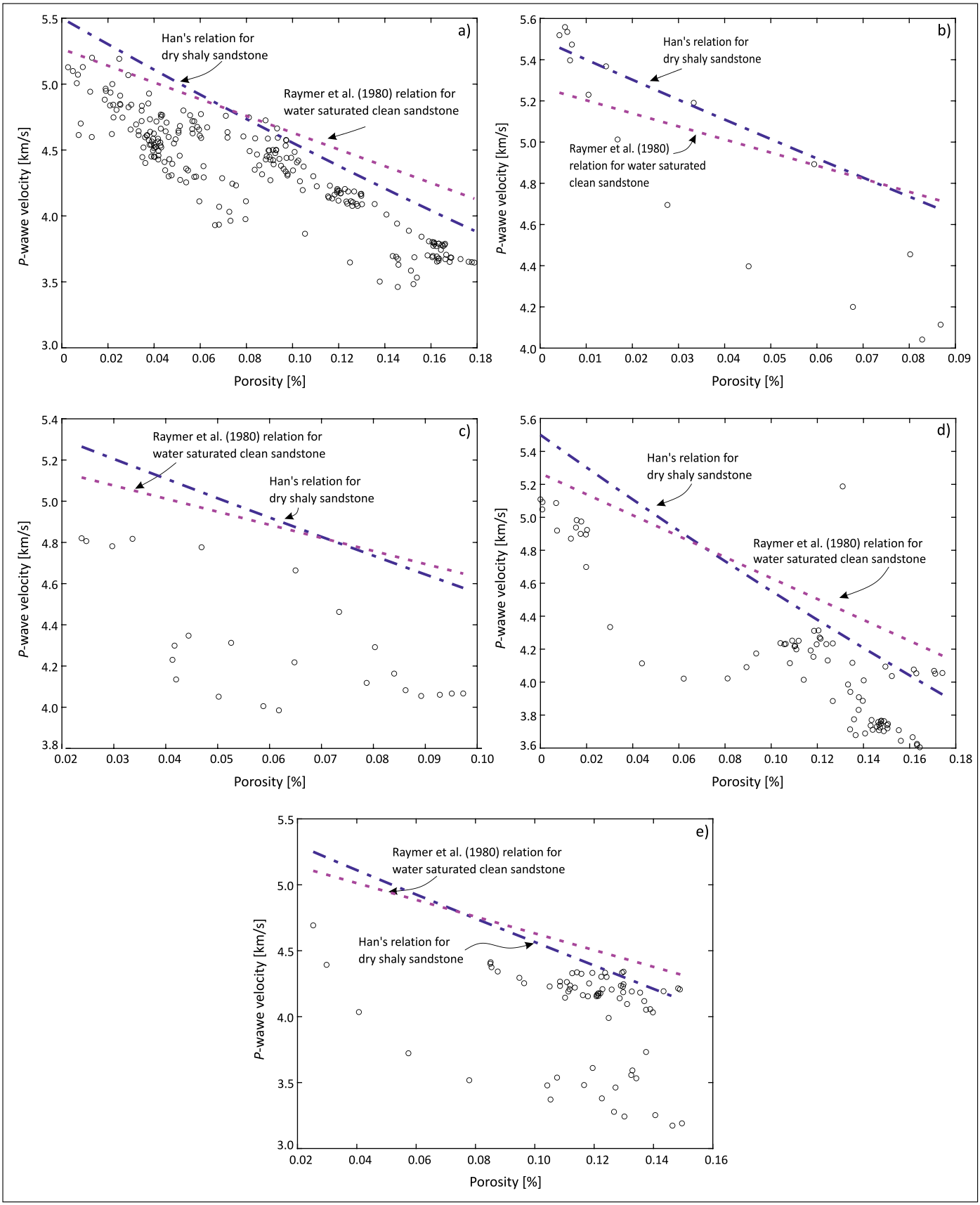

Figure 9. Velocity vs porosity crossplot of Dhodak-05 for a) zone 1 (1940–1970 meters), b) zone 2 (1970–1972 meters), c) zone 3 (1982–1985 meters), d) zone 4 (2000–2010 meters), and e) zone 5 (2033–2042 meters) with derived data (blue and purple lines)

Rysunek 9. Wykres krzyżowy prędkości i porowatości dla a) strefy 1 (1940–1970 m), b) strefy 2 (1970–1972 m), c) strefy 3 (1982–1985 m), d) strefy 4 (2000–2010 m) i e) strefy 5 (2033–2042 m) z danymi pochodnymi (linie: niebieska i fioletowa) – otwór Dhodak-05

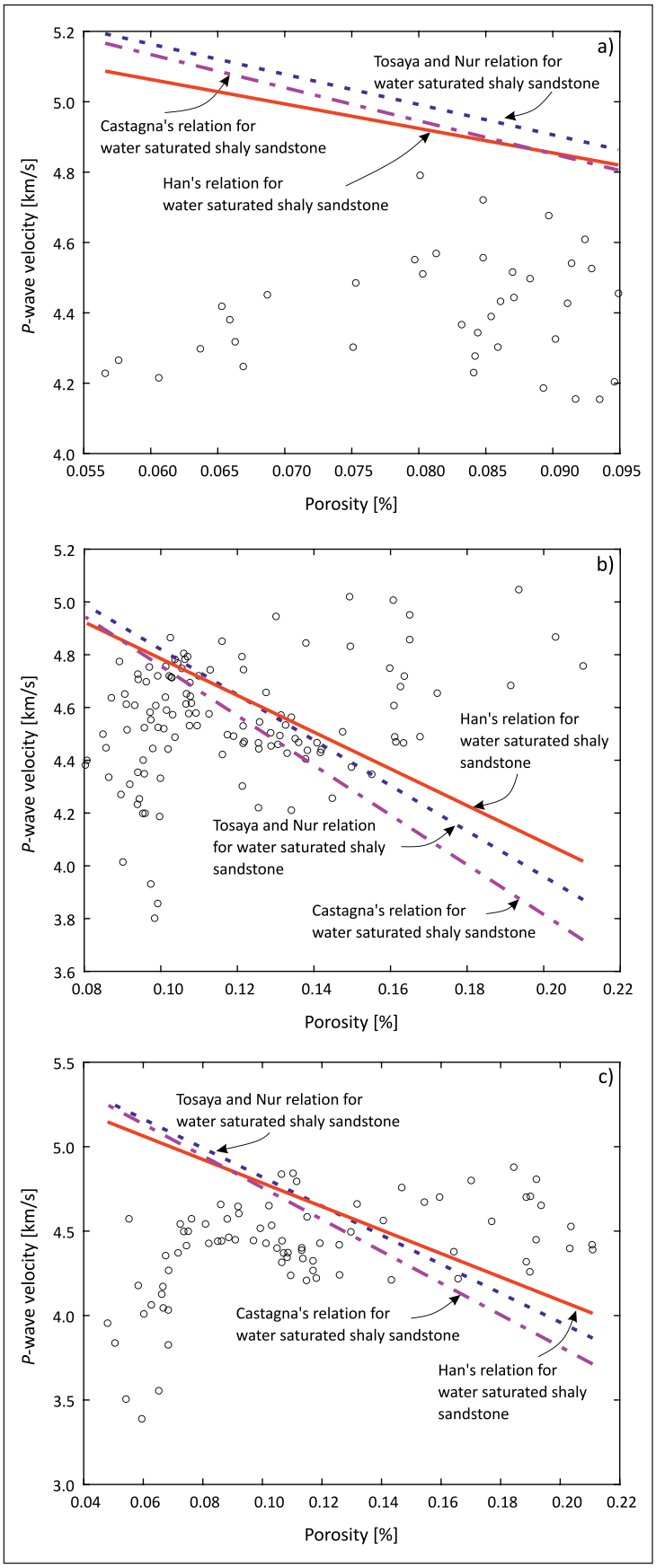

Figure 10. Velocity vs porosity crossplot of Dhodak-01 for a) zone 1 (2080–2095 meters), b) zone 2 (2100–2110 meters), and c) zone 3 (2120–2124 meters) with derived data (red, blue and purple lines)

Rysunek 10. Wykres krzyżowy prędkości i porowatości dla a) strefy 1 (2080–2095 m), b) strefy 2 (2100–2110 m) i c) strefy 3 (2120–2124 m) z danymi pochodnymi (linie: czerwona, niebieska i fioletowa) – otwór Dhodak-01

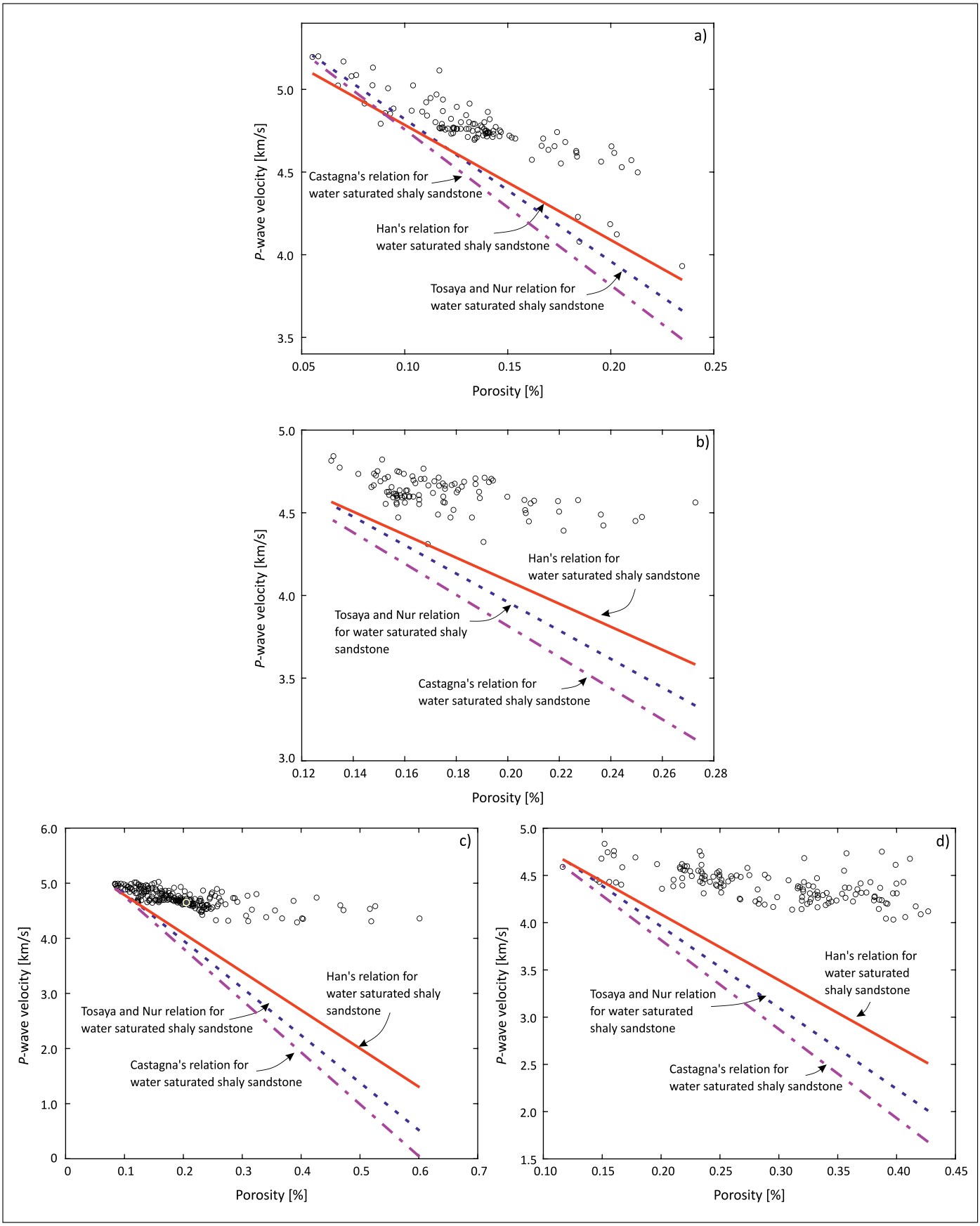

Figure 11. Velocity vs porosity crossplot of Dhodak-03 for a) zone 1 (2330–2343 meters), b) zone 2 (2352–2364 meters), c) zone 3 (2377–2404 meters), and d) zone 4 (2418–2450 meters) with derived data (red, blue and purple lines)

Rysunek 11. Wykres krzyżowy prędkość i porowatość dla a) strefy 1 (2330–2343 m), b) strefy 2 (2352–2364 m), c) strefy 3 (2377–2404 m) i d) strefy 4 (2418–2450 m) z danymi pochodnymi (linie: czerwona, niebieska i fioletowa) – otwór Dhodak-03

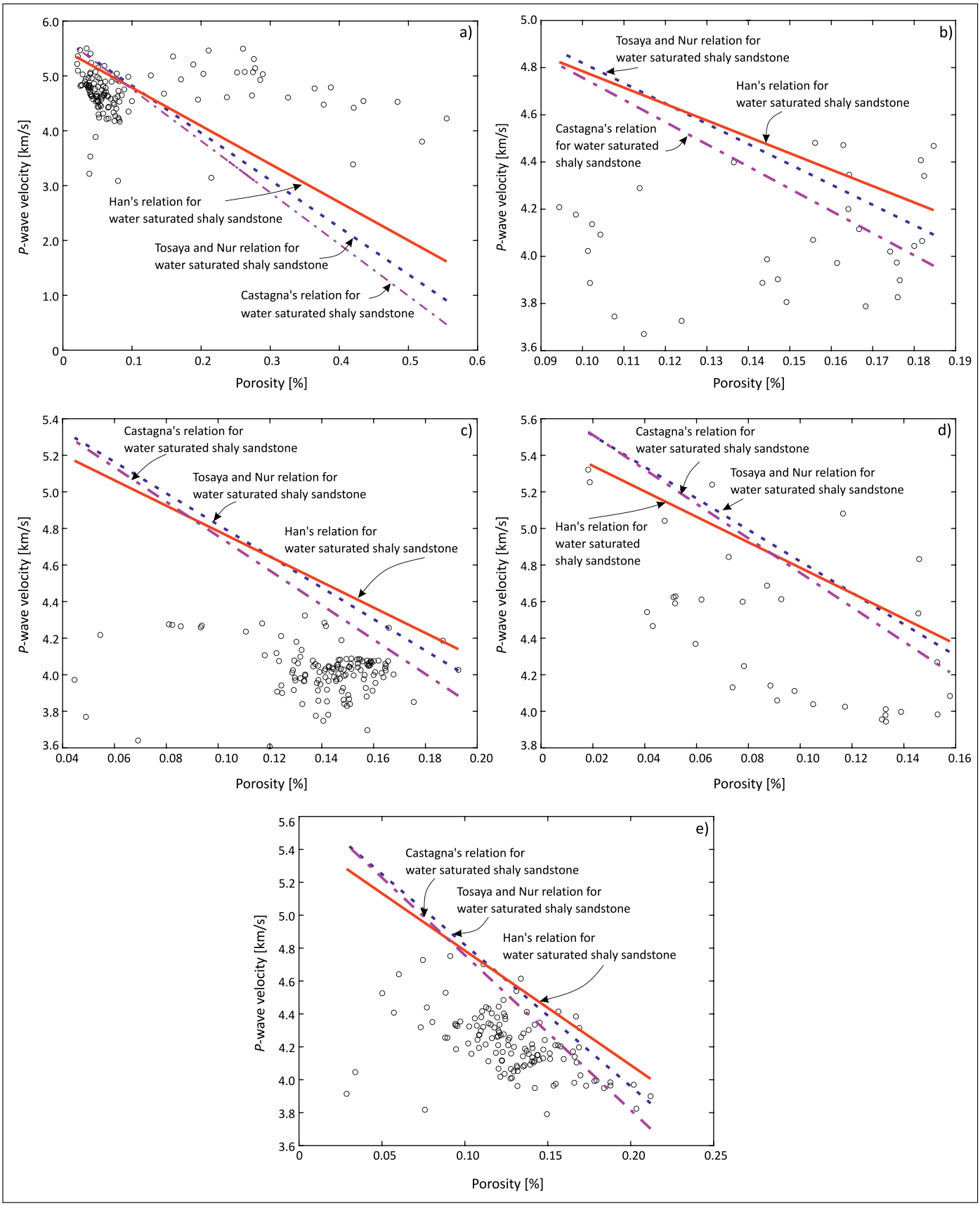

Figure 12. Velocity vs Porosity crossplot of Dhodak-04 for a) zone 1 (1990–2010 meters), b) zone 2 (2020–2025 meters), c) zone 3 (2070–2090 meters), d) zone 4 (2110–2115 meters), and e) zone 5 (2125–2145 meters) with derived data (red, blue and purple lines)

Rysunek 12. Wykres krzyżowy prędkości i porowatości dla a) strefy 1 (1990–2010 m), b) strefy 2 (2020–2025 m), c) strefy 3 (2070–2090 m), d) strefy 4 (2110–2115 m) i e) strefy 5 (2125–2145 m) z danymi pochodnymi (linie: czerwona, niebieska i fioletowa) – otwór Dhodak-04

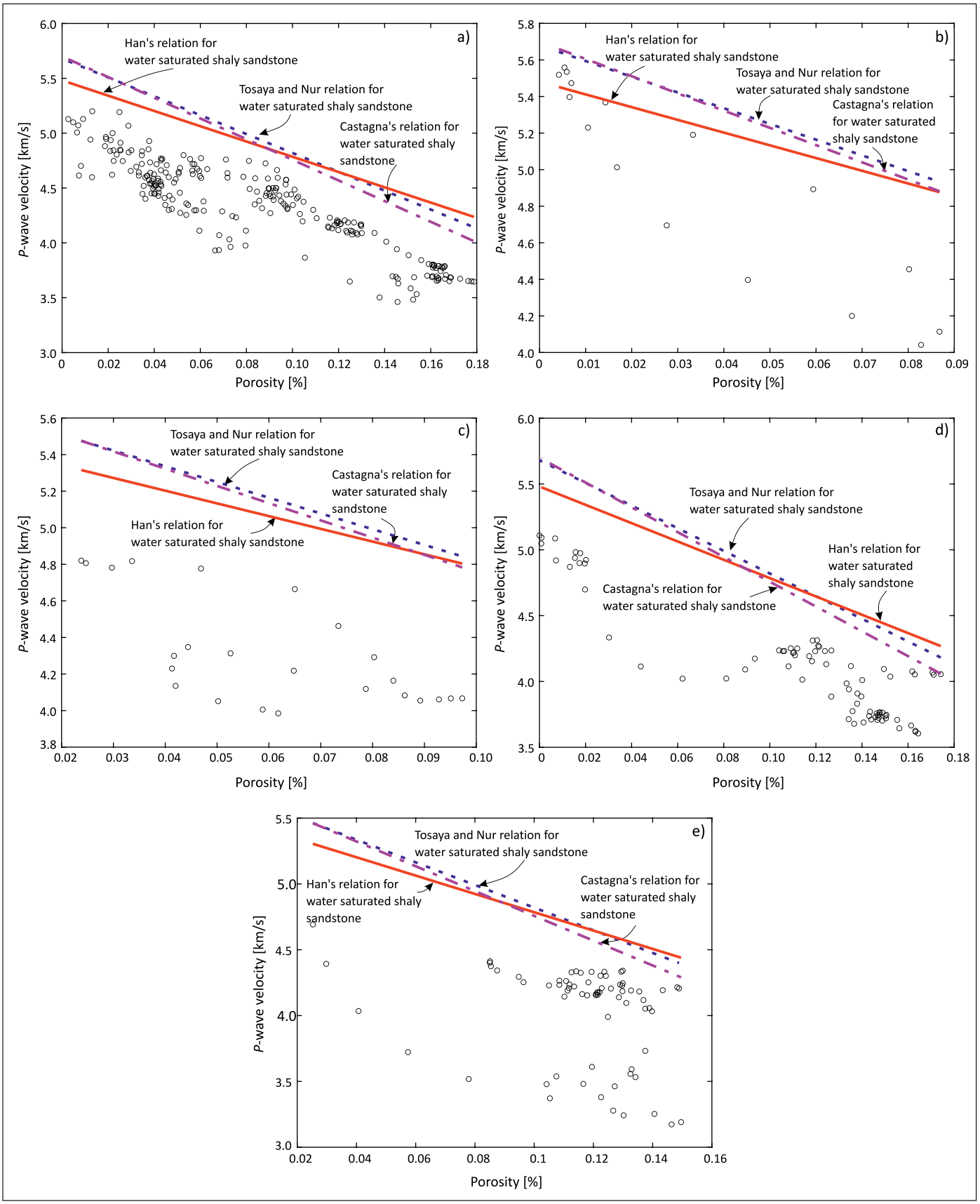

Figure 13. Velocity vs Porosity crossplot of Dhodak-05 for a) zone 1 (1940–1970 meters), b) zone 2 (1970–1972 meters), c) zone 3 (1982–1985 meters), d) zone 4 (2000–2010 meters), and e) zone 5 (2033–2042 meters) with derived data (red, blue and purple lines)

Rysunek 13. Wykres krzyżowy prędkości i porowatości dla a) strefy 1 (1990–2010 m), b) strefy 2 (2020–2025 m), c) strefy 3 (2070–2090 m), d) strefy 4 (2110–2115 m) i e) strefy 5 (2125–2145 m) z danymi pochodnymi (linie: czerwona, niebieska i fioletowa) – otwór Dhodak-05

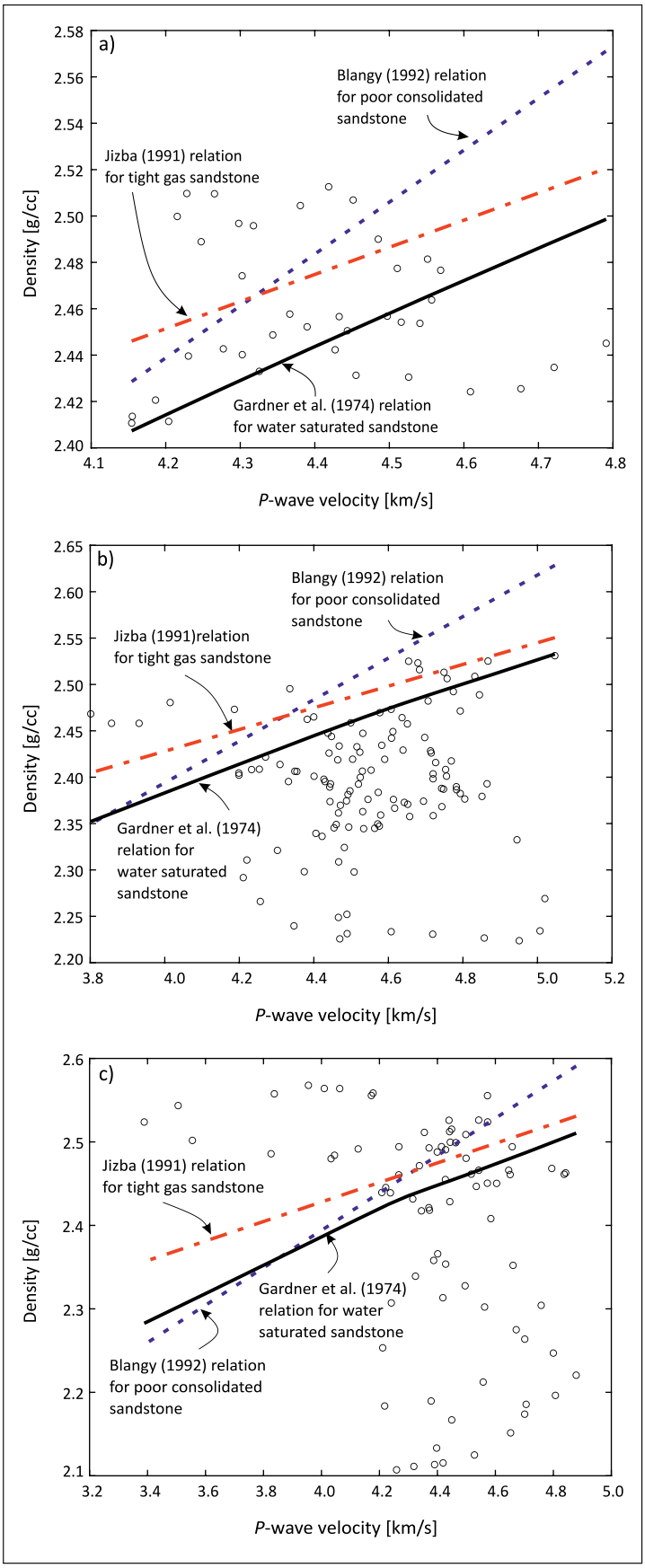

Figure 14. Density vs velocity crossplot of Dhodak-01 for a) zone 1 (2080–2095 meters), b) zone 2 (2100–2110 meters), c) zone 3 (2120–2124 meters), with derived data (blue, red and black lines)

Rysunek 14. Wykres krzyżowy gęstości i prędkości dla a) strefy 1 (2330–2343 m), b) strefy 2 (2352–2364 m), c) strefy 3 (2377–2404 m) i d) strefy 4 (2418–2450 m) z danymi pochodnymi (linie: niebieska, czerwona i czarna) – otwór Dhodak-03

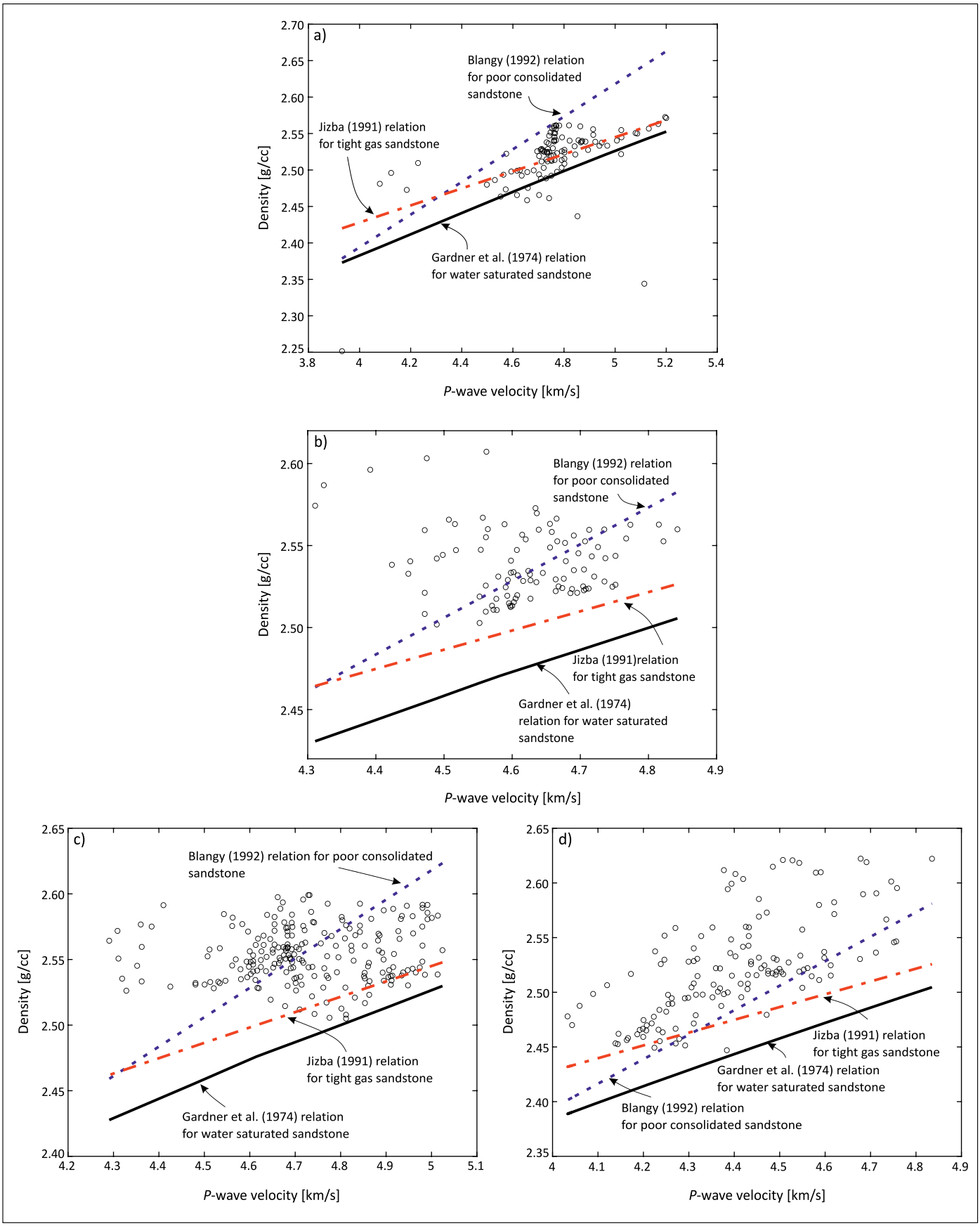

Figure 15. Density vs velocity crossplot of Dhodak-03 for a) zone 1 (2330–2343 meters), b) zone 2 (2352–2364 meters), and c) zone 3 (2377–2404 meters), d) zone 4 (2418–2580 meters) with derived data (blue, red and black lines)

Rysunek 15. Wykres krzyżowy gęstości i prędkości dla a) strefy 1 (2080–2095 m), b) strefy 2 (2100–2110 m) i c) strefy 3 (2120–2124 m) z danymi pochodnymi (linie: niebieska, czerwona i czarna) – otwór Dhodak-01

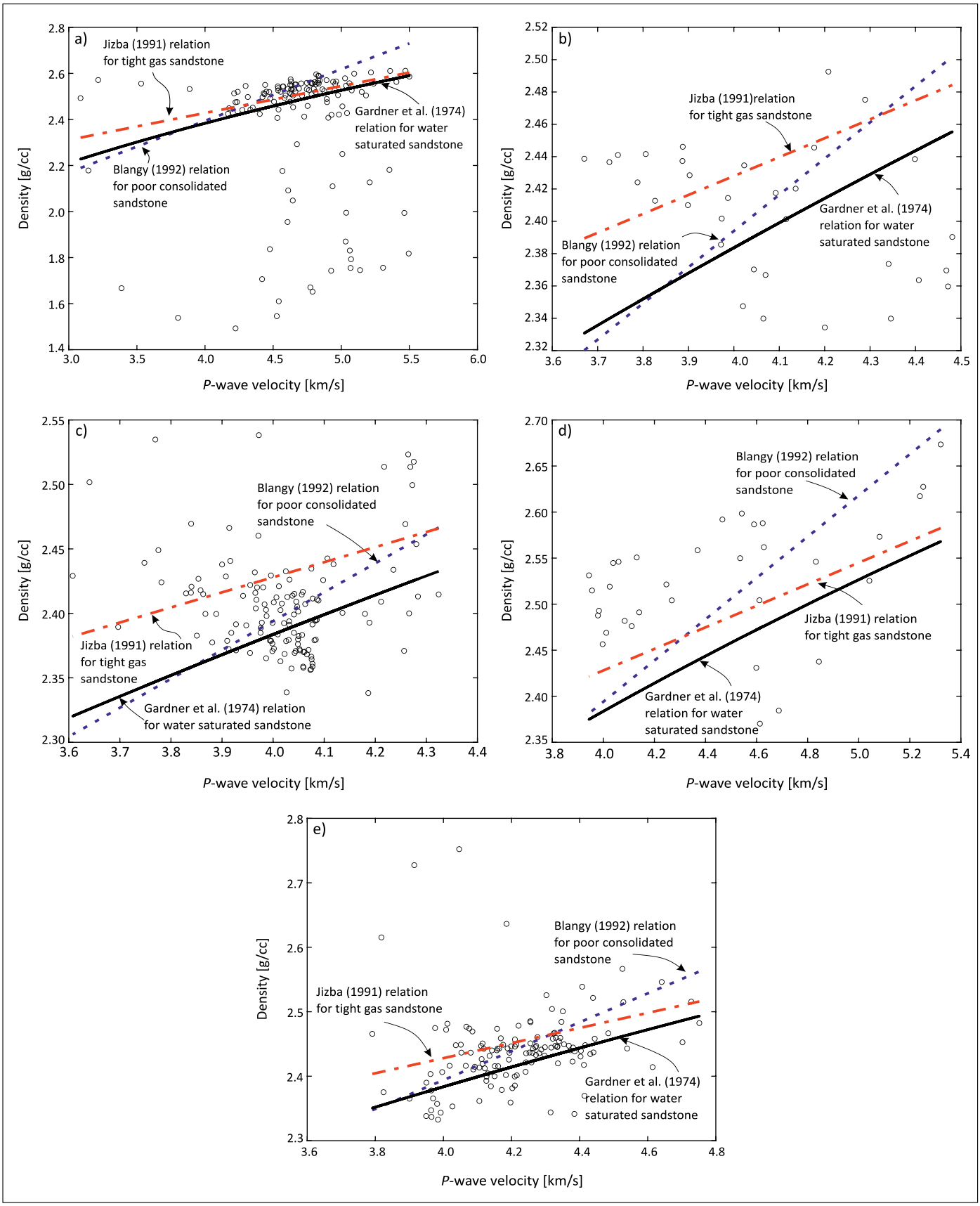

Figure 16. Density vs velocity crossplot of Dhodak-04 for a) zone 1 (1990–2010 meters), b) zone 2 (2020–2025 meters), c) zone 3 (2070–2090 meters), d) zone 4 (2110–2115 meters), and e) zone 5 (2125–2145 meters) with derived data (blue, red and black lines)

Rysunek 16. Wykres krzyżowy gęstości i prędkości dla a) strefy 1 (1990–2010 m), b) strefy 2 (2020–2025 m), c) strefy 3 (2070–2090 m), d) strefy 4 (2110–2115 m) i e) strefy 5 (2125–2145 m) z danymi pochodnymi (linie: niebieska, czerwona i czarna) – otwór Dhodak-04

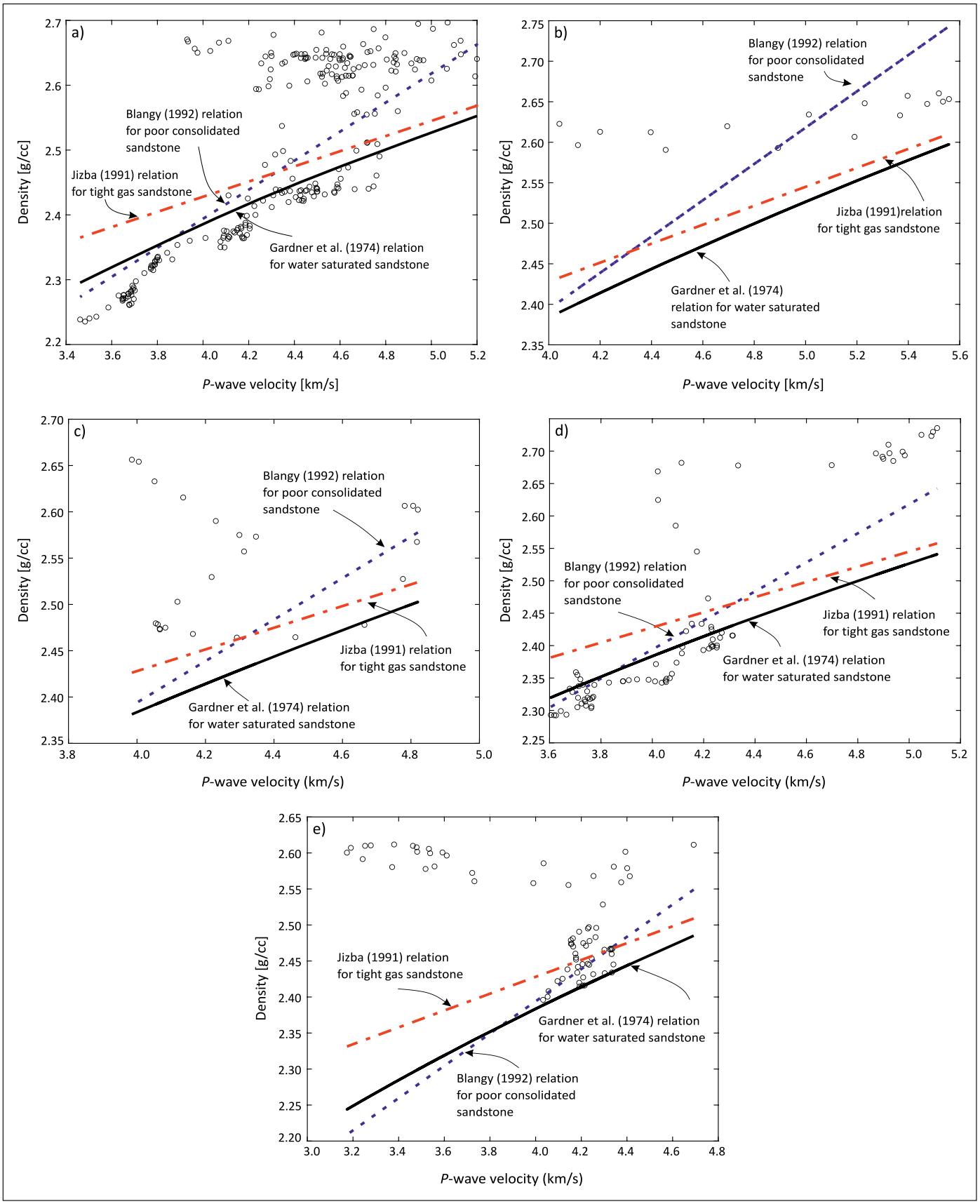

Figure 17. Density vs velocity crossplot of Dhodak-05 for a) zone 1 (1940–1970 meters), b) zone 2 (1970–1972 meters), c) zone 3 (1982–1985 meters), d) zone 4 (2000–2010 meters), and e) zone 5 (2033–2042 meters) with derived data (blue, red and black lines)

Rysunek 17. Wykres krzyżowy gęstości i prędkości dla a) strefy 1 (1940–1970 m), b) strefy 2 (1970–1972 m), c) strefy 3 (1982–1985 m), d) strefy 4 (2000–2010 m) i e) strefy 5 (2033–2042 m) z danymi pochodnymi (linie: niebieska, czerwona i czarna) – otwór Dhodak-05

Velocity-Density crossplot

The crossplot of the Pab Sandstone between the *P*-wave and density log data is shown in Figures 14, 15, 16, and 17. In these cross plots, standard Gardner's relation for water-saturated sandstone, Jizba's relation for tight gas sandstone and Blangy's relation for poorly consolidated sandstone were calculated and superimposed for different zones. Blangy's relation/model over-predicts the plotted data which means the zones are not poorly consolidated sandstone, and the Gardner's model under-predicts the plotted data which shows the zones are not water-saturated. While the Jizba's model predicts the data accurately, showing the zones are a tight gas sandstone.

Conclusions

Petrophysical interpretation of Pab Formation concluded that the average volume of shale is 34% and effective porosity is 8% for the zone ranging from 2330–2343 meters. The zone ranging 2352–2364 meters has an average volume of shale of 35% and an effective porosity 11%. Zone 1 has an average volume of shale of 38%, effective porosity of 12%. Zone 2 has an average volume of shale of 38%, and an effective porosity of 13%. The values of porosity stand good as compared to other fields surrounding the study area.

The rock physics models for the cross-plotted data (*Vp* vs porosity and density vs *Vp*) of Pab Formation show that the zone within 2330–2343 meters is not water-saturated but rather is hydrocarbon saturated and tight gas sandstone. The zones within 2352–2364 and 2377–2404 meters are poorly consolidated sandstone in places where velocity and density are increasing and a very little but negligible portion is tight gas sandstone where velocity is high and density is low. In addition to that the rock physics models for the cross-plotted data (*Vp* vs porosity and density vs *Vp*) of Pab Formation for the zone within 2418–2430 meters show that it is not water saturated but rather hydrocarbon saturated and little portion of the zone is poorly consolidated where velocity and density have a gradual increase in relation to each other.

The rock petrophysics parameters interpretation concluded that Pab Formation is a good reservoir rock for hydrocarbon accumulation, where different zones can be saturated with hydrocarbons.

Acknowledgments

This manuscript is a part of the MS research work of Mr. Irfan. The authors are thankful to the National Centre of Excellence in Geology for providing seismic data and the Geophysics Laboratory facility for the processing of data.

References

Agbauduta E.A., 2014. Evaluation of in-fill well placement and optimization using experimental design and genetic algorithm. *Master's Thesis Report, Petroleum Engineering Department, African University of Science and Technology, Nigeria*.

Amit K., Zhiling G., 2012. Applied fuzzy logic approach to inter-graded qualitative survey data into Traditional MCDM. *Hawaii International Conference on System Sciences*.

Avseth P., Mukerji T., Mavko G., Dvorkin J., 2010. Rock-physics diagnostics of depositional texture, diagenetic alterations, and reservoir heterogeneity in high porosity siliclastic sediments and rocks-A review of selected models and suggested workflows. *Geophysics*, 75(5): 75A31–75A47. DOI: 10.1190/1.3483770.

Bhaskar B., Bhadoria R.S., Yadav A.S., 2013. Transportation system of coal distribution: A fuzzy logic approach using MATLAB. *Corona Journal of Science and Technology*, 2(3): 20–30.

Blangy J.P., 1992. Integrated Seismic Lithologic Interpretation: The Petrophysical Basis. *Ph.D. Dissertation, Stanford University*.

Boah E.A., Kondo O.K.S., Borsah A.A., Brantson E., 2019. Critical evaluation of infill well placement and optimization of well spacing using the particle swarm algorithm. *Journal of Petroleum Exploration and Production Technology*, 9(4): 3113–3133. DOI: 10.1007/s13202-019-0710-1.

Cao C., Gu X., Xin Z., 2010. Stochastic chance constrained mixed-integer nonlinear programming models and the solution approaches for refinery short-term crude oil scheduling problem. *Applied Mathematical Modeling*, 34(11): 3231–3243. DOI: 10.1016/j.apm.2010.02.015.

Castagna J.P., Batzle M.L., Eastwood R.L., 1985. Relationship between compressional wave and shear wave velocities in clastic silicate rocks. *Geophysics*, 50(4): 571–581. DOI: 10.1190/1.1441933.

Castagna J.P., Batzle M.L., Kan T.K., 1994. Offset-dependent reflectivity – Theory and practice of AVO analysis. [In:] Castagna J.P., Backus M.M. (Eds.). Rock physics – the link between rock properties and AVO response. *Investigations in Geophysics*, 8 135–171.

da Veiga L.B., Lipnikov K., Manzini G., 2014. The Mimetic Finite Difference Method for Elliptic Problems, volume 11 of MS&A – Modeling, Simulation and Applications. *Springer*. DOI: 10.1007/978-3-319-02663-3.

Draege A., Johansen T.A., Brevik I., Draege C.T., 2006. A strategy for modeling the diagenetic evolution of seismic properties in sandstones. *Petroleum Geosciences*, 12(4): 309–323.

Emujakporue G., Nwankwo C., Nowasu L., 2012. Integration of well logs and seismic data for prospect evaluation of an X-field, onshore Niger Delta, Nigeria. *International Journal of Geosciences*, 3(24): 872–877. DOI: 10.4236/ijg.2012.324088.

Forth S.A., 2006. An efficient overloaded implementation of forward mode automatic differentiation in MATLAB. *ACM Trans Math Software*, 32(2): 195–222. DOI: 10.1145/1141885.1141888.

Gardner G.H.F., Gardner L.W., Gregory A.R., 1974. Formation velocity and density: the diagnostic basics for stratigraphic traps. *Geophysics*, 39(6): 770–780.

Han D., 1986. Effects of porosity and clay content on acoustic properties of sandstones and unconsolidated sediments. *Ph.D. Dissertation, Stanford University*.

Humayon M., Akram M., Malik M.R., 2012. Dhodak Field: A case history of first and largest condensate discovery of Pakistan. *AAPG Search and Discovery*, 20147.

Jizba D.L., 1991. Mechanical and Acoustic Propoerties of sandstone and shales, Volume 45 of Standford rock physics and borehole

project. *Department of Geophysics, School of Earth Sciences publishers, Standford University*.
Kearey P., Brooks M., Hill I., 2002. An Introduction to Geophysical Exploration. *Blackwell Science Ltd., Oxford*.
Khan S., Hanif M., Ali S., Nisar B.U., Latif K., Jan I.U., Pasha A.R., 2015. Lithological interpretation of middle Miocene Gaj Formation, Indus Offshore, Pakistan. *Journal of Himalayan Earth Sciences*, 48(2): 108–116.
Lie K.-A., 2016. An Introduction to Reservoir Simulation Using MATLAB User Guide for the MATLAB. Reservoir Simulation Toolbox (MRST). *SINTEF ICT, Department of Applied Mathematics, Oslo, Norway*.
Mahmood M.F., Shakir U., Abuzar M.K., Khan M.A., Khattak N.M., Hussain H.S., Tahir A.R., 2017. Probabilistic neural network approach for porosity prediction in Balkassar area: A case study. *Journal of Himalayan Earth Sciences*, 50(1A): 111–120.
Margrave G., Lamoureux M., 2019. Numerical Methods of Exploration Seismology: With Algorithms in MATLAB. *Cambridge University Press*. DOI: 10.1017/9781316756041.
Mavko G., Mukerji T., Dvorkin J., 2009. The Rock Physics Handbook, Tools for Seismic Analysis of Porous Media. *Cambridge University Press*. DOI: 10.1017/CBO9780511626753.
Moghal M.A., Saqi M.I., Hameed A., Bugti M.N., 2007. Subsurface Geometry of Potwar Sub-basin in relation to Structuration and Entrapment. *Pakistan Journal of Hydrocarbon Research*, 17: 61–72.
Moore H., 2009. MATLAB for Engineers. *Prentice Hall*.
Naseer M., Khoso T., Alam M.S., Amin S., Saqib M., 2007. Formation Pressure Prediction Using Seismic Inversion Technique in Central Indus Basin, Pakistan. *Proceedings of the ATC Conference, Islamabad, Pakistan*, 85–88.
Nazeer A., Solangi S.H., Brohi I.A., Usmani P., Napar L.D., Jahangir M., Hameed S., Ali S.M., 2013. Hydrocarbon Potential of Zindapir Anticline, Eastern Sulaiman Fold Belt, Middle Indus Basin, Pakistan. *Pakistan Journal of Hydrocarbon Research*, 22(23): 73–84.
Okwu M.O., Nwachukwu A.N., 2019. A review of fuzzy logic applications in petroleum exploration, production and distribution operations. *Journal of Petroleum Exploration and Production Technology*, 9: 1555–1568.
Okwu M.O., Olufemi A., 2018. A comparative study of artificial neural network (ANN) and adaptive neuro-fuzzy inference system (ANFIS) model in distribution system with non-deterministic inputs. *International Journal of Engineering and Business Management SAGE*, 10(12): 1–17. DOI: 10.1177/1847979018768421.
Raymer L.L., Hunt E.R., Gardner J.S., 1980. An improved sonic transit Time-to-porosity transform. *Proceedings of Society of Petrophysicists and Well-Log Analysts, Houston*, 1–13.
Souza J., Rostirolla S.R., 2011. A fast MATLAB program to estimate the multifractal spectrum of multidimensional data: Application to fractures. *Computers and Geosciences*, 37(2): 241–249. DOI: 10.1016/j.cageo.2010.09.001.
Ullah K., Arif M., Shah M.T., 2006. Petrography of sandstones from the Kamlial and Chinji formations, southwestern Kohat plateau, NW Pakistan: implications for source lithology and paleoclimate. *Journal of Himalayan Earth Sciences*, 39: 1–13.
Ullah S., Jan I.U., Hanif M., Latif K., Mohibullah M., Sabba M., Sabba M., Anees A., Ashraf U., Thanh H.V., 2022. Paleoenvironmental and bio-sequence stratigraphic analysis of the cretaceous pelagic carbonates of eastern Tethys, Sulaiman range, Pakistan. *Minerals*, 12(8): 946. DOI: 10.3390/min12080946.

Sarfraz KHAN, Ph.D.
Assistant Professor at the National Centre
of Excellence in Geology, University of Peshawar
Rahat Abad, Peshawar, 25130, KP, Pakistan
E-mail: *sarfraz_nceg@uop.edu.pk*

Muhammad Rizwan MUGHAL, Ph.D.
Assistant Professor at the Department of Meteorology
COMSATS University Islamabad
Park Rd, Chak, Tarlai Kalan, Islamabad, 45550,
Pakistan
E-mail: *rizwan.mughal@comsats.edu.pk*

Shuja ULLAH, Ph.D.
Research Assistant at the National Centre
of Excellence in Geology, University of Peshawar
Rahat Abad, Peshawar, 25130, KP, Pakistan
E-mail: *shujageo@gmail.com*

Irfan
Student at the National Centre of Excellence
in Geology, University of Peshawar
Rahat Abad, Peshawar, 25130, KP, Pakistan
E-mail: *irfan_buner21@yahoo.com*

Umair Bin NISAR, Ph.D.
Assistant Professor at the Centre for Climate
Research and Development, COMSATS University
Islamabad
Park Rd, Chak, Tarlai Kalan, Islamabad, 45550,
Pakistan
E-mail: *Umair.nisar@comsats.edu.pk*

Shahid NAWAZ
Student at the National Centre of Excellence
in Geology, University of Peshawar
Rahat Abad, Peshawar, 25130, KP, Pakistan
E-mail: *shahid.quaid@gmail.com*

Waqas AHMED, Ph.D.
Associate Professor at the National Centre
of Excellence in Geology, University of Peshawar
Rahat Abad, Peshawar, 25130, KP, Pakistan
E-mail: *waqas.nce@gmail.com*

Nazir Ur REHMAN, Ph.D.
Assistant Professor at the Department of Geology,
Khushal Khan Khattak University Karak
Karak, 27200, KP, Pakistan
E-mail: *nazirurrehman@kkkuk.edu.pk*